

Participation of Eu-aggregates in the photoluminescence, afterglow and thermoluminescence of UV-irradiated KCl:Eu at 20 K

This article has been downloaded from IOPscience. Please scroll down to see the full text article.

2005 J. Phys.: Condens. Matter 17 181

(<http://iopscience.iop.org/0953-8984/17/1/016>)

View [the table of contents for this issue](#), or go to the [journal homepage](#) for more

Download details:

IP Address: 129.252.86.83

The article was downloaded on 27/05/2010 at 19:31

Please note that [terms and conditions apply](#).

Participation of Eu-aggregates in the photoluminescence, afterglow and thermoluminescence of UV-irradiated KCl:Eu at 20 K

S Alvarez-García¹ and T M Pitters²

¹ Programa de Doctorado en Ciencias (Física), Universidad de Sonora, PO Box 5-088, 83190 Hermosillo, Mexico

² Departamento de Investigación en Física, Universidad de Sonora, PO Box 5-088, 83190 Hermosillo, Mexico

E-mail: salvarez@cajeme.cifus.uson.mx and pitters@cajeme.cifus.uson.mx

Received 18 August 2004, in final form 4 November 2004

Published 10 December 2004

Online at stacks.iop.org/JPhysCM/17/181

Abstract

The participation of different aggregated phases of the Eu impurity in the afterglow (AG) and thermoluminescence (TL) of KCl:Eu after UV-irradiation at 20 K is investigated. Several aggregated phases of Eu are formed by applying different thermal treatments and their formation is monitored by photoluminescence. It is shown that the treatments leading to high concentration of aggregates result in much higher AG and TL yields than the treatments leading to high concentration of dipoles. This is due to a more efficient AG and TL production for aggregates than for dipoles. Additionally, we observed a huge increase of the AG and TL production efficiency around dipoles after ageing at 200 °C. The results are discussed in view of a recently proposed mechanism for AG based on the migration of H centres through dislocation lines. The main conclusions are that dislocation lines trap dipoles and that precipitation occurs along dislocation lines causing a large fraction of aggregates to participate in the AG and TL.

1. Introduction

The creation of defects by ionizing radiation in alkali halide crystals has been extensively investigated over the last forty years and our knowledge about the mechanism is well documented [1]. Upon ionization the hole is immediately self-trapped forming a V_k centre. When an electron is attracted to the V_k centre, it forms a self-trapped-exciton (STE). The STE relaxes spontaneously to an off-centre configuration which is effectively a nearest neighbour F–H pair. If the H centre migrates farther from the F centre, then the pair becomes stable.

The introduction of divalent cation impurities, like Eu^{2+} ions, in the alkali halide lattice enhances significantly the formation of radiation defects such as F–H centre pairs [2–5]. This effect has been explained by different mechanisms:

- (i) the inhibition of the F–H recombination by trapping the H centre at the divalent impurity–cation vacancy dipole ($\text{Me}^{2+}-v_c$ dipole) or at dipole aggregates,
- (ii) the enhanced generation of F–H centre pairs near the $\text{Me}^{2+}-v_c$ dipole or dipole aggregates, and
- (iii) the direct participation of the Me^{2+} ion as a hole-trap or electron-trap centre.

Furthermore, the F–H centre pair formation efficiency is affected by the thermal history of the crystal [6] which has been ascribed to the precipitation of the divalent cation impurity into different phases [7, 8].

The creation of stable defects is also observed in Eu-doped alkali halide crystals exposed to UV light with an energy lower than that of the exciton absorption band. This phenomenon has been attributed to an electron transfer process from the disturbed anion lattice around the Eu^{2+} impurity followed by the formation of a V_k centre in the vicinity of the Eu^{2+} and the emission of the electron [9]. The V_k -electron relaxation process results in the formation of a trapped exciton close to the impurity whose decay leads to the creation of an F–H centre pair. The F–H separation necessary for AG and TL was assigned to the expulsion of the H centre during the STE relaxation. The TL was associated with the thermal release of the trapped H centres followed by their recombination with F centres, and the AG to an electron–hole tunnelling mechanism in which the electron tunnels from the F centre to the H centre. Recently, however, an alternative mechanism for F–H centre separation which explains the AG decay at too low temperatures for H centre migration, has been proposed [10, 11]. In this mechanism the separation of an F–H centre pair created in the vicinity of the Eu related defect was associated with the migration of the H centre through a dislocation line pinned at the Eu related defect. The AG was explained by the not trapped migrating H centres which return to their corresponding F centres. It was demonstrated that this mechanism indeed results in an AG with a similar decay curve as that predicted by the theory of tunnelling.

In this paper, the participation of the different precipitated phases of the Eu impurities in the AG and TL phenomena in KCl:Eu irradiated at low temperature (20 K) with non-ionizing UV light is investigated. In order to identify the participating aggregates, the emission spectra related to PL, AG and TL were analysed. For the interpretation of the results, the mechanism of migrating H centres through dislocation lines is adopted as a working hypothesis. The possible participation of dislocation lines in the precipitation process is discussed within this hypothesis.

2. Experimental details

Samples of typical size of about $5 \times 5 \times 1 \text{ mm}^3$ were cleaved from a single crystal of KCl doped with EuCl_2 (200 ppm), grown in the Instituto de Física de la Universidad Nacional Autónoma de México by the Czochralski method. For the temperature treatments the samples were wrapped in Al foil and placed into a pre-heated furnace (THERMOLYNE, model 1310). After remaining there for the desired period, the samples were taken out and quickly cooled down by pressing them onto a copper block at RT. For the PL, AG and TL measurements the sample was tied to the cold finger of a two stage cryogenic helium refrigerator (APD, model DE-202) with a thin wire. In this way we avoided the use of vacuum grease as a paste compound from which we have observed a persistent luminescence in the wavelength range

of the sample emission. In a previous work, this luminescence was erroneously interpreted as fast decaying AG [12].

The temperature of the cold finger was measured by an Au–constantan thermocouple and controlled by two resistors mounted close to the sample. The cold finger with sample was enveloped in a vacuum shroud with four quartz windows for optical access and was introduced into the sample compartment of a spectrofluorometer (SPEX, model FLUOROMAX). The excitation source was a 450 W Xe arc-lamp (ORIEL, model 6262). The excitation light was blocked by a homemade shutter and monochromated by a monochromator (KRATOS, model GM252). From the monochromator output, the light was guided through a high-grade fused silica fibre (ORIEL, model 77578) to the sample compartment of the spectrofluorometer. The luminescence of the sample was collected by the emission detection system of the fluorometer. The temperature of the photomultiplier in the detection system was kept constant with an external water circulator at 15 °C to reduce background fluctuations. The setup was automated to perform sequences of PL (during irradiation), AG (immediately after irradiation) and TL (during heating at a rate of 0.1 K s⁻¹ up to 300 K after waiting 300 s for reducing the AG signal) for different excitation and irradiation wavelengths between 200 and 400 nm. All the PL and AG emission spectra were measured at 20 K to obtain a better discrimination between peaks. The emission spectra were corrected for the background signal and the detector response. After converting them from wavelength to energy scale, they were deconvoluted into a set of Gaussian peaks by the non-linear square fitting option of some commercial software (Origin 7.0).

3. Experimental results

3.1. Photoluminescence

The PL emission spectra of a single sample of KCl:Eu exposed to successive thermal treatments are shown in figure 1 (right column). In treatment (A) the sample was stored at RT for several years; then, it was heated at 500 °C for 1 h (treatment B), and finally it was aged at 200 °C for around 300 h (treatment C). These treatments are known to produce several precipitation states of the Eu impurity which have been associated with different PL emission peaks at RT [7, 8]. Our analysis of the PL at 20 K showed that all emission spectra after the different thermal treatments could be fitted with a single set of 10 Gaussian peaks. The peak parameters are listed in table 1.

During the fitting procedure, it was appreciated that the intensity of some peaks seems to maintain a constant ratio independent of excitation wavelength and thermal treatment. This fact can be interpreted as excessive peak decomposition. To confirm this, the fitting process was done again using the same peak parameters but with a proportionality constraint between the intensity of adjacent peaks which were suspected to be dependent. In the new fitting process, the constraints were accepted by most of the emission curves allowing us to conclude that the groups of peaks (LT1–LT2), (LT3–LT4) and (LT7–LT8–LT9) form single emission bands. Peaks LT5 and LT6 also presented a constant intensity ratio but with a different value for each thermal treatment and therefore were considered independent. The emission spectra are thus composed of six independent bands of which some of them are non-Gaussian. They are further labelled as BD1 to BD6 (see convolution band curves in inset of figure 2 and band parameters in table 1).

The PL excitation spectrum of almost all emission bands shown in figure 2 present the two well-known bands related to transitions between the ground state and the excited states E_g (200–270 nm) and T_{2g} (320–400 nm) of the Eu²⁺ ion in a cubic crystal field. The high energy

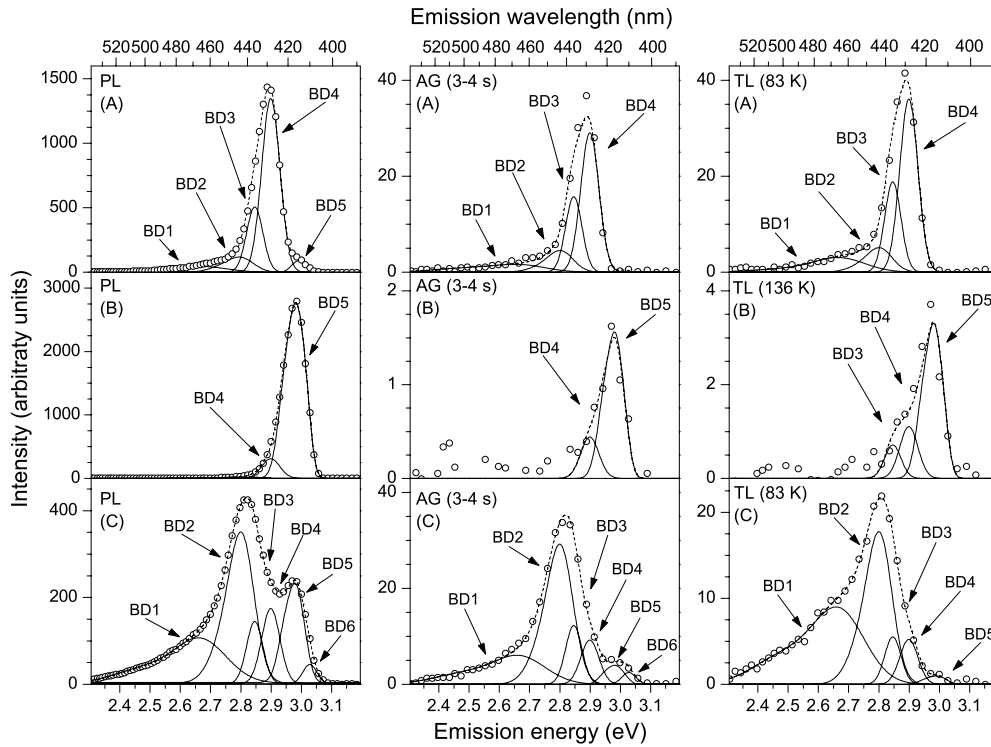


Figure 1. Emission spectra at 20 K of PL exposed to 325 nm light, and of AG and TL induced by 235 nm light in KCl:Eu after different thermal treatments (A: several years at RT, B: 1 h at 500 °C and C: 300 h at 200 °C). The AG spectra correspond to 3–4 s after the end of the irradiation and TL spectra to an intermediate temperature during the heating at constant rate to RT. Open circles represent the experimental data, continuous curves the individual emission bands and dashed curves the convoluted fitting curve. Spectra were corrected by the response of the detection system.

Table 1. Fitting parameters of the emission bands of the PL at 20 K in KCl:Eu. Each band is composed of one or more Gaussian peaks. Peak parameters x_c and w are defined by the fitting Gaussian function: $y(x) = A \exp(-(x - x_c)^2/2w^2)$, where x is the photon energy in eV. The amplitude A of each peak (LT) is taken such that the convoluted band amplitude (BD) is unity.

Band	Peak	x_c (eV)	w (eV)	A
BD1	LT1	2.490 ± 0.050	0.103 ± 0.018	0.430
	LT2	2.670 ± 0.030	0.084 ± 0.020	0.895
BD2	LT3	2.766 ± 0.024	0.053 ± 0.003	0.377
	LT4	2.8076 ± 0.0018	0.039 ± 0.004	0.708
BD3	LT5	2.846 ± 0.018	0.027 ± 0.007	1
BD4	LT6	2.899 ± 0.009	0.030 ± 0.006	1
BD5	LT7	2.952 ± 0.018	0.026 ± 0.020	0.549
	LT8	2.987 ± 0.066	0.021 ± 0.005	0.692
	LT9	3.0164 ± 0.0016	0.018 ± 0.001	0.263
BD6	LT10	3.028 ± 0.020	0.023 ± 0.015	1

band in the excitation spectra seems to be composed of at least two peaks around 230 and 260 nm. However, the excitation spectrum of BD1 only presents the 230 nm peak, suggesting that this peak as well as BD1 is not related to a transition in the Eu^{2+} ion but possibly to one

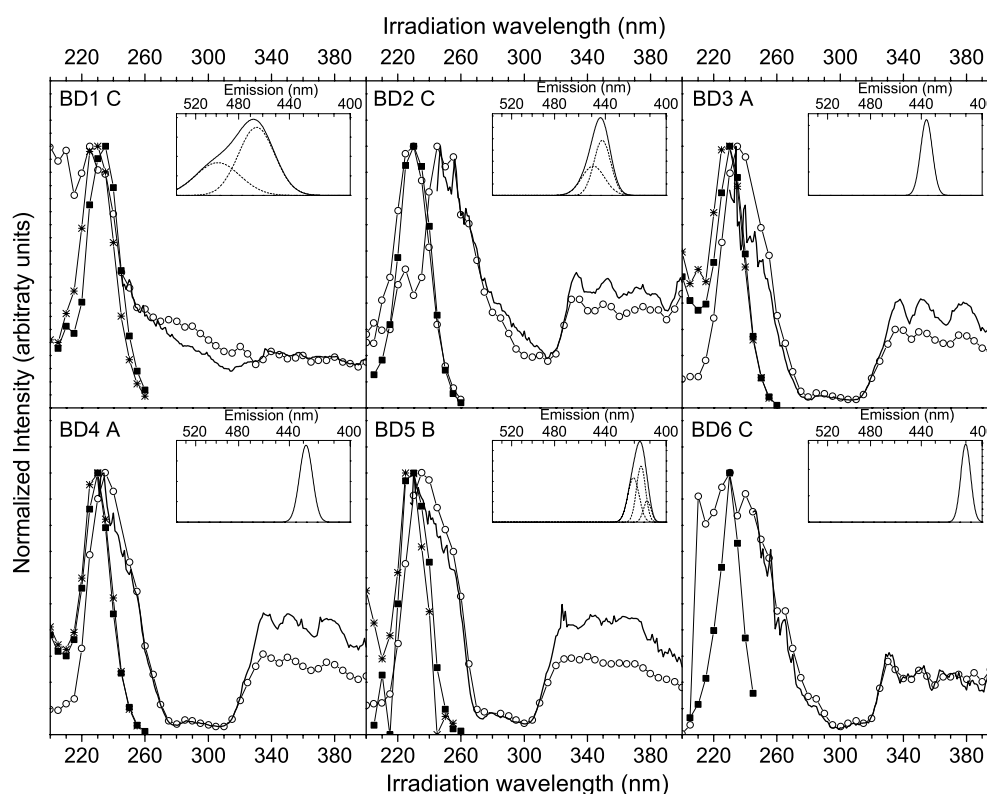


Figure 2. Excitation spectra of the PL and creation spectra of the AG and TL after exposure to UV-visible light at 20 K for the six emission bands in the thermal treatment where they dominate. Open circles represent the PL, solid squares the AG and stars the TL for the same sample. Solid curves represent the PL in a different sample for comparison. The excitation spectra were corrected by the emission of the irradiation lamp and the response of the detection system. The insets show the convolution of the corresponding emission bands.

in a structural defect close to it. Therefore we suppose that only the 260 nm peak is a part of the excitation to the E_g state.

Emission BD2 was clearly identified in treatment (C) and according to the conclusions of Rubio *et al* [8] would be assigned to the metastable precipitated EuCl_2 phase. Emission bands BD3 and BD4 dominate in (A). Band BD3 has a central position close to one of the metastable EuCl_2 precipitated phases previously reported [8], but its width is too narrow. In any case, the relative great separation of the Eu excitation bands suggests an assignment to some Eu precipitate. Based on its central position, width and dominating presence in the well-aged crystal at RT, it is tempting to assign band BD4 to the Suzuki precipitated phase. However the thermal solvation of this phase occurs at temperatures lower than 150 °C [7] which contradicts the presence of band BD4 after treatments (B) and (C). A possible explanation for this is that band BD4 in treatments (B) and (C) is associated with trimers of which the emission is similar to that of the Suzuki phase as suggested by Martinaga *et al* [13]. Although trimers are also unstable at temperatures around 150–200 °C, they could be formed from dipoles and dimers during the not too-fast cooling down to RT because trimers are formed considerably faster than the Suzuki phase. Emission band BD5 dominates in treatment (B) where it is known that the Eu impurities are in the $\text{Eu}-v_c$ dipole configuration, clearly giving the assignment of

Table 2. Assignment of the 6 emission bands of KCl:Eu at 20 K. Band centre in eV- and nm-units and the FWHM value are shown for each band. The thermal treatment in which each band dominates are included (A: several years at RT, B: 1 h at 500 °C and C: 300 h at 200 °C). Previously reported data for the PL at RT are included for comparison (* widths not reported for the KCl:Eu crystal where taken from similar identified peaks in the NaCl:Eu [8]).

Band	Centre (nm)	Centre (eV ⁻¹)	FWHM (eV)	Dominate in treatment	Tentative assignment	Reference
BD1	468	2.654	0.282	C	Structural defect close to the Eu ion	This work
	478	2.597	0.30*	C	Metastable EuCl ₂ phase	[8]
BD2	443	2.80	0.109	C	Metastable EuCl ₂ phase	This work
	439	2.83	0.22*	C		[8]
BD3	436	2.846	0.064	A	Some Eu phase	This work
BD4	428	2.899	0.071	A	Suzuki phase and/or Eu-v _c trimers	This work
	427	2.908	0.17	A	Suzuki phase	[7]
BD5	417	2.981	0.083	B	Eu-v _c dipoles and dimers	This work
	419	2.963	0.15	B		[7]
BD6	410	3.028	0.054	C	Stable EuCl ₂ phase	This work
	410	3.028	0.13*	C		[8]

the band. It also appears in other treatments indicating that the dipole configuration was not completely lost by ageing. Emission band BD6 only appears in (C) and its central position around 410 nm suggests its association with a stable EuCl₂ phase [8]. Table 2 compares our data and assignments of the PL emission bands at 20 K with that of the PL emission bands at RT previously reported.

3.2. Afterglow and thermoluminescence after irradiation at 20 K

The deconvolution of the emission spectra of AG and the low temperature TL peaks (up to 83 K) could be performed satisfactory with the same six independent bands identified in the PL spectra. The high temperature TL emission spectra show small deviations between measured and fitted curves which are probably due to the temperature dependence of the peak widths. Figure 1 compares the typical emission spectra of the PL, AG and TL observed in a KCl:Eu sample submitted to treatments A, B and C. In general, afterglow emission is much more intense after ageing (treatments A and C) than after quenching (treatment B). This is partly due to the fact that the AG production is more efficient around aggregates than around dipoles. However the efficiency of AG production around dipoles also seems to increase during ageing at 200 °C, as can be seen as follows. The AG intensity of a band divided by its PL intensity can be taken as a relative measure of the efficiency of AG production. Using this measure it can be calculated that the AG generation of BD5 (dipoles) is about 30 times more efficient after treatment C than after treatment B.

The band intensities in the TL emission spectra behave in a similar way as those in the AG with respect to the different thermal treatments. However, spectra after treatment C show that the contribution of Eu-precipitate bands relative to that of the dipole band is lower in the AG than in the TL. This suggests that the fraction participating in AG of created defects around Eu-aggregates is lower than that of created defects around dipoles.

Following the intensity of each band at different irradiation wavelengths, the creation spectra of the AG and TL were generated (figure 2). The creation spectrum for AG and TL

appears identical for all emission bands and does not depend on thermal treatment. There exists one peak centred around 230 nm. This peak seems to be the same as that in the PL excitation spectra which was not related to a transition of the Eu ion but probably to one close to the Eu ion. The Eu emission induced by the excitation of the 230 nm peak would thus be due to some energy transfer process from the defect recombination site to the Eu ion. These considerations agree with a recently proposed model in which the initial process of the UV induced creation of F and H centres takes place at the disturbed lattice around the Eu impurity [9].

4. Discussion and conclusions

Both AG and TL phenomena imply the migration of the H centre from the creation site. Assuming that dislocation lines act as guides for migration, then the defects close to dislocation lines would be more efficient in the production of AG and TL. In view of this, the increase of AG and TL production efficiency around dipoles after treatment C suggests that dislocation lines trap dipoles at 200 °C. Furthermore the higher efficiency of aggregates compared to free dipoles suggests that aggregation takes place mainly along dislocation lines. This can be understood if we assume that the trapped dipoles are still free to move along the dislocation lines, allowing the aggregation to occur.

The relative higher efficiency of aggregates in TL than in AG compared to dipoles could be explained by a difference in the recombination probability. Although the relation between both AG and TL yield and recombination probability is not completely clear, it seems reasonable to assume that lower recombination probability results in relatively higher TL yield because the H centres that do not recombine during AG will contribute to TL. This suggests that the F–H recombination in the presence of an aggregate is lower than in the presence of a dipole. The reason for different F–H probabilities could be that the initial process of the F–H centre formation is followed by a relaxation of the ‘F centre’–‘impurity defect’–‘dislocation line’ complex to a different configuration for each type of aggregate. The shape of the AG decay is not much affected by changes in the recombination probabilities [11], therefore the observed similarity of the AG decay of each band does not contradict this idea.

In summary, we come to the following picture of the processes responsible for precipitation, AG and TL: dipoles are trapped by dislocation lines but remain mobile along them. Consequently, the formation of aggregates takes place mainly in dislocation lines. The initial process for the creation of F and H pairs (responsible for AG and TL) is the same for all aggregates and not related to a transition on the Eu^{2+} ion but to one on a nearby structural defect. After the initial process, the H centre migrates randomly through the dislocation line while the F centre, the Eu-phase and the dislocation line relax to a configuration, dependent on the Eu-phase involved. The H centre may return to the F centre and recombine (AG) or may trap at some defect located near or at the dislocation line (leading to TL). The recombination probability of an F–H centres pair is lower in a Eu-configuration of aggregates than of dipoles. This causes a relatively lower AG production efficiency for aggregates.

Acknowledgments

This work has been partially supported by CONACyT under contract number 3873-E, 37641-E, U40497-F and J35222-E. We are grateful to Dr H Riveros for supplying the crystals and to J C Ávila-Barrera for his technical support.

References

- [1] Song K S and Williams R T 1996 *Self-Trapped Excitons (Springer Series in Solid-State Sciences vol 105)* (Berlin: Springer) p 123, 130
- [2] Chowdari B V R and Itoh N 1971 *Phys. Status Solidi b* **46** 549
- [3] Kao K J and Perlman M M 1979 *Phys. Rev. B* **19** 1196
- [4] Rubio J O, Aguilar M G, Lopez F J, Galan M, Garcia-Sole J and Murrieta H S 1982 *J. Phys. C: Solid State Phys.* **15** 6113
- [5] Opyrchal H, Nierzewski K D, Macalik B and Mladenova M 1986 *Phys. Status Solidi b* **135** 141
- [6] Rubio J O, Flores M C, Murrieta H S, Hernandez J A, Jaque F and Lopez F J 1982 *Phys. Rev. B* **26** 2199
- [7] Lopez F J, Murrieta H S, Hernandez J A and Rubio J O 1980 *Phys. Rev. B* **22** 6428
- [8] Rubio J O, Murrieta H S, Hernandez J A and Lopez F J 1981 *Phys. Rev. B* **24** 4847
- [9] Babin V, Krasnikov A and Zazubovich S 2003 *Radiat. Eff. Defects Solids* **158** 227
- [10] Alvarez-Garcia S, Pitors T M and Barboza-Flores M 2001 *Radiat. Meas.* **33** 813
- [11] Pitors T M and Alvarez-Garcia S 2002 *Radiat. Eff. Defects Solids* **157** 705
- [12] Alvarez-Garcia S and Pitors T M 2003 *Radiat. Eff. Defects Solids* **158** 281
- [13] Matinaga F M, Nunes L A O, Zilio S C and Castro J C 1988 *Phys. Rev. B* **37** 993